

# Mitigating Uncertainty of Classifier for Unsupervised Domain Adaptation

Shanu Kumar  
Microsoft, India

shankum@microsoft.com

Vinod K Kurmi  
IIT Kanpur

vinodkk@iitk.ac.in

Praphul Singh  
Oracle, India

praphul.singh@oracle.com

Vinay P Namboodiri  
University of Bath

vpn22@bath.ac.uk

## Abstract

Understanding unsupervised domain adaptation has been an important task that has been well explored. However, the wide variety of methods have not analyzed the role of a classifier’s performance in detail. In this paper, we thoroughly examine the role of a classifier in terms of matching source and target distributions. We specifically investigate the classifier ability by matching a) the distribution of features, b) probabilistic uncertainty for samples and c) certainty activation mappings. Our analysis suggests that using these three distributions does result in a consistently improved performance on all the datasets. Our work thus extends present knowledge on the role of the various distributions obtained from the classifier towards solving unsupervised domain adaptation.

## 1. Introduction

Efficacy of using deep neural networks for solving a variety of problems in computer vision has been well established [18, 12, 31, 3]. These models are trained on large datasets and work in a variety of real-world settings. However, it has been shown [41] that even after being trained on large datasets, these models suffer from inferior performance when they are used on data that differ for reasons such as background clutter, distribution of classes and illumination and pose conditions. To address this mismatch in performance, there has been a large body of work that aims to reduce the covariate shift by adapt features using unsupervised domain adaptation [29, 45]. However, these techniques proposed so far have mainly ignored the response of the classifiers. They have focused on aligning the feature representations between the source and target domains that are input to the classifiers. In our work, we argue that such an approach under-utilizes the use of the classifier. Through this work, we analyse the role of the classifier and observe that carefully matching the classifier’s response for source

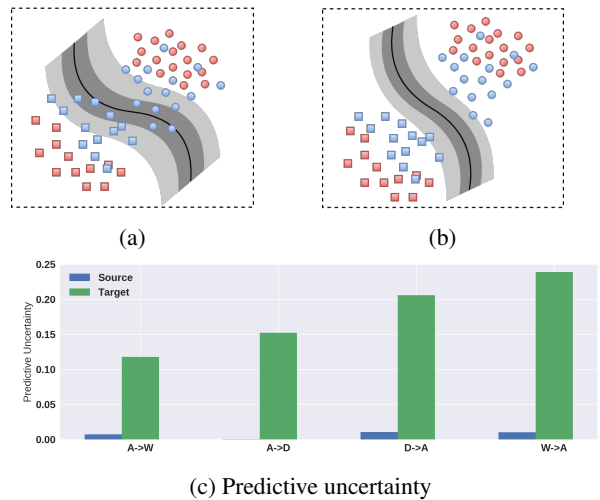


Figure 1: Comparison of adversarial feature adaptation and our proposed method (red: source domain and blue: target domain). (a) The mean and variance of the decision boundary are not correctly approximated for the target domain, due to this all the samples of decision boundary do not separate most target domain examples. (b) Our approach learns better approximation of the mean and variance of the decision boundary and also learns more class-discriminative feature representations for the target domain. (c) Predictive uncertainty estimates of the target domain is relatively much higher than of the source domain images after only adapting the distribution of features on *Office-31* dataset (AlexNet). For A→D, uncertainty in the source domain is almost 0.

and target domains can result in consistent improvement in performance and lower uncertainty in the target domain.

In order to understand the existing dominant approach adopted by most classifiers, we need to understand the underlying assumption. Most of the existing works in domain adaptation [24, 9, 42] have focused on learning domain-

invariant feature representations. They work on the assumption that the classifier learned in the source domain can be used in the target domain after feature adaptation. This theory is based on the principle that the posterior of the classifier in the target domain may be similar to the posterior learned in the source domain. But this may not be true always as the label-feature distribution can differ for the source and target domain. In figure 1a, we illustrate an instance where the feature representations are domain-invariant and yet, the features in the target domain are not class-discriminative for the classifier learned in the source domain. As the classifier is only trained on the source domain, all the decision boundaries sampled from the posterior of the classifier entirely separates both classes in the source domain. Even though features are domain invariant, every sampled decision boundary do not separate both the classes in the target domain which results in lower performance and higher uncertainty. We observe similar pattern after performing adversarial adaptation of features for  $W \rightarrow A$  task using AlexNet. The features shown in the figure 2a are domain-invariant. In the figure 2b, we can verify that features of the source domain images form unique class clusters but all the features of the target domain images are not class discriminative. The tools we use to analyze this performance are based on probabilistic uncertainty measures [6, 17] and certainty activation mappings [19]. Recently, there have been a few methods that have focused on classifier adaptation [38, 47, 23]. [38] addressed this issue by incorporating conditional entropy loss which refines the decision boundary, while [23] enables the adaptation by generating transferable examples to fill in the gap between the source and target domains. However, we believe that they have not sufficiently addressed this problem.

In this paper, we solve the problem by learning a better approximation of the posterior of the classifier in the target domain. This is challenging as we cannot approximate the true posterior of the classifier without the class labels. We propose an unsupervised method that jointly aligns three specific distributions across domains. In our analysis, we observed that there is higher predictive uncertainty in the target domain as compared to the source domain. Also, there is a domain shift in the probability distribution of the classifier, which strengthens our belief that the mean of the posterior of the classifier is not correctly approximated in the target domain. Recently, [19] has proposed certainty activation mappings that highlight the regions where the classifier is certain during predictions. We observe that certainty activation mappings in the source domain highlight class-discriminative regions, but in the target domain due to high uncertainty, these mappings do not highlight class-discriminative regions. This suggests that the approximation of the variance of the posterior is also not correct in the target domain. Based on these findings,

we propose Triple Distribution Matching for Domain Adaptation (TDMDA), which jointly matches the distribution of feature representations, probability distributions, and certainty activation mappings from the target domain to that of the source domain. The main contributions of this paper are summarized as follows:

- We investigate the limitations of the traditional adversarial feature adaptation methods based on predictive uncertainty, probability distribution, and certainty activation mappings.
- We propose TDMDA for learning a better approximation of the posterior of the classifier in the target domain by jointly matching three distributions.
- We provide the evaluation of our method on various domain adaptation benchmark datasets and its comparisons with most of the state of the art methods.
- We show the effectiveness of our method by providing an empirical analysis using the estimates of predictive uncertainty and various visualizations.

## 2. Related Work

**Domain Adaptation:** There has been a wide variety of feature adaptation techniques for solving unsupervised domain adaptation. Early approaches were based on feature alignment through estimation of divergence between distributions such as MMD [43, 24, 49], CORAL [39], CCD and Wasserstein metric [37]. Ganin et al.[8] enable the model to learn both class-discriminative and domain invariant representations by training a discriminator in an adversarial way. Other approaches such as [36, 42, 41] have also proposed methods based on adversarial domain adaptation. More recent methods [13, 34, 14, 2] have performed unpaired image-to-image translation using generative adversarial networks (GAN) [10] by generating synthetic images of one domain in other. Attention based approaches have been also applied in domain adaptation. TADA [46] uses entropy of the local and global discriminators for finding transferable regions which are also used as attention for classifier. In CADA [19], attention is obtained by discriminator’s certainty activation mappings and are used to focus on more discriminative regions. Huang *et al*[15] shows that there is domain discrepancy in the classifier by visualizing attention mechanism. They propose to align the distributions of activations of intermediate layers of source and target to adapt the classifier. We also propose a similar idea except the self attention or class activation mappings, we align certainty activation mappings.

Along with feature adaptation, few approaches have explored adaptation of classifier. Shu *et al.* [38] propose decision-boundary refinement via conditional entropy loss. They have also incorporated domain adversarial training which penalizes violation of the cluster assumption. [23]

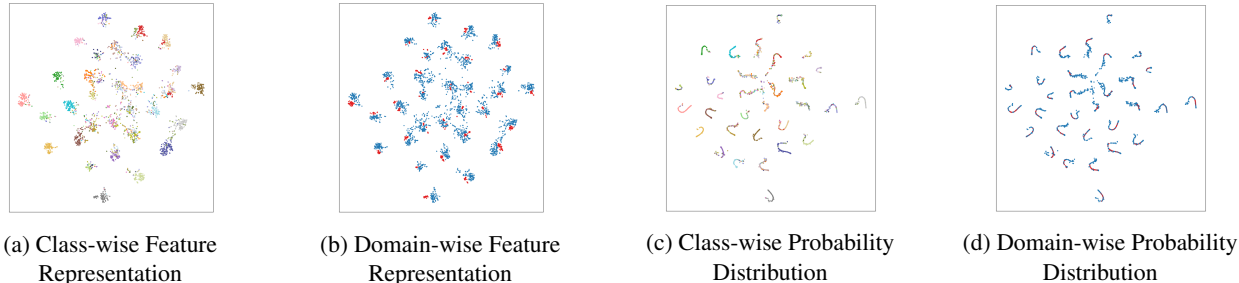


Figure 2: Domain-wise and Class-wise t-SNE visualization of feature and probability distribution after preforming adversarial feature adaptation on Office31 dataset (Source: W and Target: A) using AlexNet. The distribution of feature representation is domain-invariant after performing feature adaptation but many target domain features are not class-discriminative. In the probability distribution, we can observe domain shift between the target and source domain data points. We also have provided the magnified version of these plots in the supplementary material.

encourages adaptation of classifier by generating transferable adversarial examples. Similarly, [20] uses adversarial dropout to learn discriminative features by pushing the decision boundary away from the target domain’s features. [5] also aligns the class conditional distribution of features of source and target domain. These have however, not studied classifier’s distributions thoroughly as proposed in this work. We analyze it and provide a more general framework that considers various distributions for the classifier and jointly matches them to enforces both class-discriminative features and lower uncertainty in target domain.

**Uncertainty Estimation:** Our method relies on the various uncertainty estimation techniques that have been investigated. We provide an overview of the literature in this area. Bayesian neural networks (BNN) have been used in a wide variety of tasks for estimating predictive uncertainty. But determining the exact inference of  $p(\mathbf{Y}|\mathbf{X})$  is an intractable problem because computing the posterior expression  $p(\theta|\mathbf{X}, \mathbf{Y}) = p(\mathbf{Y}|\mathbf{X}, \theta)p(\theta)/p(\mathbf{Y}|\mathbf{X})$  is analytically impossible. Thus the posterior  $p(\theta|\mathbf{X}, \mathbf{Y})$  is approximated by a simple distribution  $q^*(\theta)$  parameterized by  $\{\mu, \sigma\}$ . To approximate inference for deep learning models, [7] has proposed a Dropout variational inference method. In [28], it has been shown that dropout variational inference has better calibration under in-domain distribution or distributional shifts than Temp Scaling [11], SVI[1] and LL[32]. Thus, we have employed dropout variational inference for quantifying predictive uncertainty.

Based on [7], Kurmi *et al.* [19] has incorporated estimation of uncertainty for domain adaptation. They propose a method to visualize the activation mappings of certainty and uncertainty estimates. In their work, the discriminator’s certainty activation mappings are used as an attention for guiding the classifier, but the classifier uncertainty estimates, and certainty activation mappings are not investigated. As a result, the method does not ensure the discriminativity of the adapted features. This drawback is thoroughly investi-

gated and addressed in our work. [47] propose to minimize the difference of predictive uncertainty of the source and target domains, along with feature adaptation.

### 3. Probabilistic Justification for the Proposed Approach

In general, any adversarial feature adaptation method focuses only on reducing the domain shift in the feature distribution, thus making  $\mathcal{P}(F(\mathbf{X}_s)) \approx \mathcal{P}(F(\mathbf{X}_t))$ . The inference in target domain can be defined mathematically as  $\mathcal{P}(\mathbf{Y}_t|\mathbf{X}_t) = \mathcal{P}(\mathbf{Y}_t|F(\mathbf{X}_t))\mathcal{P}(F(\mathbf{X}_t))$ . Adapting the features results in  $\mathcal{P}(F(\mathbf{X}_s)) \approx \mathcal{P}(F(\mathbf{X}_t))$ . Now,  $\mathcal{P}(\mathbf{Y}_t|F(\mathbf{X}_t))$  requires evaluation of the posterior  $p(\theta_c|F(\mathbf{X}_t), \mathbf{Y}_t)$  for inference. Existing methods assume that the posterior of target-domain classifier can be approximated directly by using the posterior,  $p(\theta_c|F(\mathbf{X}_s), \mathbf{Y}_s)$  learned from the source domain. But the approximation  $q^*(\theta_c)$ , learned by using the source domain do not guarantee that  $p(\theta_c|F(\mathbf{X}_s), \mathbf{Y}_s)$  is the correct approximation of  $p(\theta_c|F(\mathbf{X}_t), \mathbf{Y}_t)$  as the class labels for the target domain are not used. Therefore, reducing the domain shift alone do not guarantee that  $\mathcal{P}(\mathbf{Y}_s|F(\mathbf{X}_s)) \approx \mathcal{P}(\mathbf{Y}_t|F(\mathbf{X}_t))$ .

#### 3.1. High Predictive Uncertainty in Target Domain

In figure 1c, we have plotted the predictive uncertainty for source and target domains after the feature adaptation in Office-31 dataset [33]. From the figure, it is evident that after the feature adaptation, there is reasonably high predictive uncertainty still present in the target domain. The reason for the high predictive uncertainty is that the parameters  $\{\mu_c, \sigma_c\}$  of the posterior  $q^*(\theta_c)$ , learned from the source domain are not the correct approximation of the posterior,  $p(\theta_c|F(\mathbf{X}_t), \mathbf{Y}_t)$  of the target domain. In the proposed method, we show that by considering the unlabeled target domain data  $\mathbf{X}_t$ , the posterior  $q^*(\theta_c)$  can be approximated better for the target domain. The result for the same is provided later in figure 6.

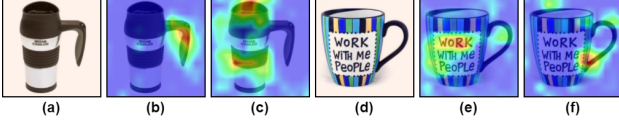


Figure 3: Visualization of certainty and uncertainty activation mappings of last convolutional layer in source domain. Uncertainty activation mappings are shown in (b) and (e) and, certainty activation mappings are shown in (c) and (f). Certainty activation mappings also highlight the class-discriminative regions of an image.

### 3.2. Domain Shift in Probability Distribution

Figure 2 shows the probability distribution after performing the adversarial adaptation of features. In figures 2d and 2c, we can see that all the data points lie on curved lines with unique class clusters in the source domain, but data points of the target domain do not follow a similar structure. Many data points in the target domain are in the center of the plot and do not correspond to any cluster. These are also not class-specific and causes a domain shift in the probability distribution  $\hat{y}_c$  of the source and target domain. Domain shift can happen if either the mean of decision boundaries do not separate the data well in the target domain or the margin between the data and mean of decision boundaries is very small in the target domain. We can assume that this is a result of incorrect approximation of the  $\mu_c$  of  $q^*(\theta_c)$ , as the classifier is trained only using source-domain labels. We can enforce better approximation of the mean,  $\mu_c$  of  $q^*(\theta_c)$  by minimizing the domain shift in the probability distribution  $\hat{y}_c$ , as we want the mean of decision boundaries to separate the classes in both domains very well with a large margin.

### 3.3. Certainty Activation Mapping

Similar to class activation mappings proposed in [35], we can compute certainty activation mappings to identify the regions where the classifier is certain for performing predictions. Like class activation mappings, certainty activation mappings are highly class-discriminative for images of the source domain. Similarly, uncertainty activation mappings lead us to the uncertain regions for the predictions. By computing both the mappings through the approach proposed in [19], we can visualize the certain and uncertain regions in the images for the classifier. This, in turn, provides much more information than the class activation mappings. In figure 3, certainty and uncertainty activation mappings are shown respectively for the source domain for Office-31 dataset. In figure 4, certainty activation mapping in the target domain is shown after adversarial adaptation of features. We can observe that the class-discriminative regions are highlighted by uncertainty activation mappings instead

of certainty activation mappings. This was not the case for the images in source domain as the posterior,  $q^*(\theta_c)$  is approximated well for the source domain. For the target domain, we are using the same posterior, which therefore results in high uncertainty and non-class discriminative certainty activation mappings.

If the variance  $\sigma_c$  of  $q^*(\theta_c)$  is not learned correctly for the target domain, it will result in the incorrect sampling of decision boundaries. These decision boundaries may not separate the data well and thus will cause higher predictive uncertainty for target domain images. Variance for the target domain cannot be directly approximated, but reducing the uncertainty or any function proportional to uncertainty can lead to a better approximation of the variance  $\sigma_c$ . A similar kind of approach has been proposed in [47], where the difference between the predictive uncertainties of source and target domain is minimized for producing consistent predictions. One important point to note is that reduction in predictive uncertainty do not necessarily mean a reduction in uncertainty on the class-discriminative regions. On the contrary, it may also be due to a higher reduction of uncertainty for the non-class discriminative regions. This brings us to an observation that learning correct explanation is better than learning correct answers.

We propose a mechanism to ameliorate the certainty activation mappings in the target domain to be class discriminative by matching the distribution of certainty activation mappings of the target domain to that of the source domain. As certainty activation mapping is a function of uncertainty, therefore this will lead to a reduction in uncertainty and finally to a better approximation of variance  $\sigma_c$  of  $q^*(\theta_c)$  in the target domain.

## 4. Methodology

In unsupervised domain adaptation, we have a source domain  $P(X_s, Y_s)$  with  $n_s$  i.i.d. labeled observations  $\{x_i^s, y_i^s\}_{i=1}^{n_s}$  and a target domain  $P(X_t, Y_t)$  with  $n_t$  i.i.d. unlabeled observations  $\{x_i^t\}_{i=1}^{n_t}$ . The goal is to learn transferable features  $f = F(x)$  and an adaptive classifier  $C$  which minimises the generalisation error on the target domain with lower uncertainty. For learning better approximation of the posterior  $q^*(\theta_c)$  for target domain, we propose Triple Distribution Matching for Domain Adaptation (TDMDA), which solves the following three tasks: (a) Feature adaptation, (b) Predictive probability adaptation and (c) Certainty Activation Mapping adaptation.

### 4.1. Feature Adaptation

Adversarial adaptation of features aims to learn both class-discriminative and domain-invariant features. Domain-invariance is achieved by training a domain discriminator  $D_f$ , which predicts the domain label for both the source and target domain features, which are generated by



Figure 4: Visualization of certainty activation mappings of the last convolutional layer in target domain after adversarial feature adaptation for A→D (AlexNet). These mappings are not highlighting any class-discriminative region.

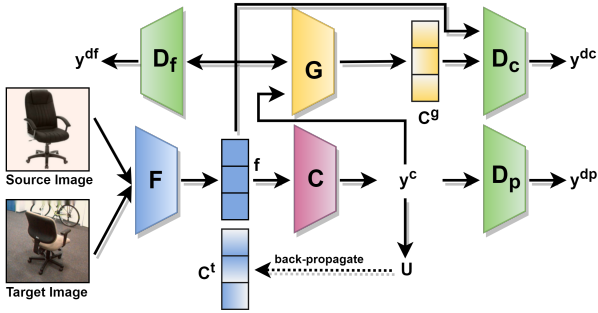


Figure 5: The architecture of Triple Distribution Matching for Domain Adaptation (TDMDA) consists of feature extractor  $F$ , Classifier  $C$ , Feature domain discriminator  $D_f$ , Probability distribution domain discriminator  $D_p$ , Certainty activation mapping domain discriminator  $D_c$  and Certainty activation mapping generator  $G$ .

training the feature extractor  $F(x_i)$ . The aim is to confuse the discriminator  $D_f$  so that it is unable to distinguish between source and target domain, thus making the feature  $f_i$  domain-invariant. The classifier  $C$  is trained to learn class discriminative features through the cross-entropy loss the source domain:

$$\mathcal{L}_c = \frac{1}{n_s} \sum_{x_i \in \mathcal{D}_s} \mathcal{L}(C(\mathbf{f}_i), y_i^s) \quad (1)$$

where  $y_i^s$  is true class label. The domain discriminator  $D_f$  is trained using the following loss:

$$\mathcal{L}_{df} = \frac{1}{n_s + n_t} \sum_{x_i \in \mathcal{D}_s \cup \mathcal{D}_t} \mathcal{L}(D_f(\mathbf{f}_i), d_i) \quad (2)$$

where  $d_i$  is the domain label. The predictive uncertainty  $U_i$  is estimated by using entropy of the average class probabilities of  $T$  Monte Carlo samples of the features.

$$p(y_{i,t}^c) = \text{Softmax}(C(\mathbf{f}_{i,t})) \quad (3)$$

$$U_i = -\frac{1}{T} \sum_{t=1}^T \sum_{c=1}^C p(y_{i,t}^c = c) * \log p(y_{i,t}^c = c) \quad (4)$$

## 4.2. Probability Distribution Adaptation

Earlier works used the mean of posterior  $\mu_c$  learned from the source domain for the posterior of the target domain. For

high-confidence predictions in the target domain, the  $\mu_c$  for the target domain needs to be approximated separately using target domain images. Therefore, we aim at minimizing the domain shift in the probability distribution  $C(\mathbf{f}_i)$  of source and target domains for learning a better approximation of the mean  $\mu_c$  of the posterior of the classifier. Similar to adversarial feature adaptation, we train a domain discriminator  $D_p$  for predicting the domain of probability distribution  $C(\mathbf{f}_i)$ . The classifier  $C$ , on the other hand, is trained to fool the discriminator by predicting high-confidence class predictions for both source and target domains. The probability distribution adaptation also results in learning more domain-invariant feature representation. The loss function for probability distribution adaptation is defined in Eq. 5.

$$\mathcal{L}_{dp} = \frac{1}{n_s + n_t} \sum_{x_i \in \mathcal{D}_s \cup \mathcal{D}_t} \mathcal{L}(D_p(C(\mathbf{f}_i)), d_i) \quad (5)$$

## 4.3. Certainty Activation Mapping Adaptation

We have followed [19] for obtaining certainty activation mappings  $\mathbf{C}_i^t$  for the classification task. We perform element-wise multiplication of feature with negative of the gradient of predictive uncertainty  $U_i$  with respect to feature. We are only interested in the features that have a positive influence on the certainty estimates i.e., pixels whose intensity should be increased in order to improve the certainty. Therefore negative activations are replaced by a large negative number  $b$ , which will become zero after applying Softmax.

$$s_i = \begin{cases} \mathbf{f}_i * -\frac{\partial U_i}{\partial \mathbf{f}_i} & \text{if } \mathbf{f}_i * -\frac{\partial U_i}{\partial \mathbf{f}_i} \geq 0 \\ b, & \text{otherwise} \end{cases} \quad (6)$$

$$\mathbf{C}_i^t = 1 + \text{Softmax}(s_i) \quad (7)$$

Certainty activation mapping highlights the class-discriminative regions in the source domain. But, for many cases in the target domain, this is not observed, and this causes a domain shift for certainty activation mappings between source and target domains. Due to the wrong approximation of the variance  $\sigma_c$  of the posterior of classifier  $C$ , there is high predictive uncertainty for the target domain as the classifier is uncertain on class-discriminative regions. To fix the issue, we propose to match the distribution of certainty activation mappings of the target domain to that of the source domain by using a domain discriminator  $D_c$ . The

classifier is trained to fool the discriminator  $D_c$  by learning a better approximation of the variance  $\sigma_c$ .

The certainty activation mapping is a function of class logits  $C(\mathbf{f}_i)$  and features  $\mathbf{f}_i$ . To fool the discriminator  $D_c$ , we need to compute the gradients of predictive uncertainty with respect to certainty activation map, which itself is a function of derivative of predictive uncertainty. This will result in the computation of second derivatives of predictive uncertainty with respect to the features. We propose a way to deal with this complexity. As Neural Networks are universal approximators, we can easily learn the certainty activation mapping function using them. Therefore, we suggest using a generator  $G$  for generating the certainty activation mappings for both source and target domains. Now, since we are generating the certainty activation mapping  $\mathbf{C}_i^g$ , we only have to deal with the first derivatives, thus making the computations simpler than before. Certainty activation mapping generator  $G$  is trained by minimizing the mean squared loss  $\mathcal{L}_g$ .

$$\mathbf{C}_i^g = G(C(\mathbf{f}_i), \mathbf{f}_i) \quad (8)$$

$$\mathcal{L}_g = \|\mathbf{C}_i^t - \mathbf{C}_i^g\|^2 \quad (9)$$

Certainty activation mapping do not provide any information without the feature or image. Therefore the discriminator  $D_c$  will have both certainty activation mappings  $\mathbf{C}_i^g$  and  $\mathbf{f}_i$  as inputs. Since we only aim to match the distribution of certainty activation mappings here, the features will act as weights for the certainty activation mappings. The discriminator  $D_c$  is trained using the loss function  $\mathcal{L}_{dc}$ .

$$\mathcal{L}_{dc} = \frac{1}{n_s + n_t} \sum_{x_i \in \mathcal{D}_s \cup \mathcal{D}_t} \mathcal{L}(D_c(\mathbf{C}_i^g, \mathbf{f}_i), d_i) \quad (10)$$

#### 4.4. Final Objective

We enable better approximation of the posterior  $q^*(\theta_c)$  in both source and target domain by Triple Distribution Matching for Domain Adaptation (TDMDA), which jointly learns class discriminative and domain invariant features, domain invariant probability distribution, and class-discriminative certainty activation mappings. The final objective function  $J$  of TDMDA is defined as:

$$J(\theta_f, \theta_c, \theta_{df}, \theta_g, \theta_{dp}, \theta_{dc}) = \mathcal{L}_c + \mathcal{L}_g - \lambda_f * \mathcal{L}_{df} - \lambda_p * \mathcal{L}_{dp} - \lambda_c * \mathcal{L}_{dc} \quad (11)$$

where  $\theta_f, \theta_c, \theta_{df}, \theta_g, \theta_{dp}, \theta_{dc}$  are the parameters of feature extractor  $F$ , classifier  $C$ , feature domain discriminator  $D_f$ , certainty activation mapping generator  $G$ , probability distribution domain discriminator  $D_p$  and certainty activation mapping domain discriminator  $D_c$  respectively.  $\lambda_f, \lambda_p, \lambda_c$  are hyper-parameters that provides a trade-off between classifier and discriminators. The optimization problem is to find the parameters  $\hat{\theta}_f, \hat{\theta}_c, \hat{\theta}_g, \hat{\theta}_{df}, \hat{\theta}_{dp}, \hat{\theta}_{dc}$  that

Table 1: Classification accuracy (%) on *Office-31* dataset for unsupervised domain adaptation (AlexNet [18])

Method	A→W	A→D	D→A	W→A	Avg
AlexNet[18]	60.6	64.2	45.5	48.3	54.65
DANN[8]	73.0	72.3	52.4	50.4	62.03
JAN[26]	75.2	72.8	57.5	56.3	65.45
MADA[30]	78.5	74.1	56.0	54.5	65.78
CDAN[25]	77.9	74.6	55.1	57.5	66.28
Entro[47]	78.9	77.8	56.6	57.4	67.68
CAT[5]	80.7	76.4	63.7	62.2	<b>70.75</b>
CADA[19]	<b>83.4</b>	80.1	59.8	59.5	70.70
TDMDA	82.6	<b>85.2</b>	<b>66.3</b>	<b>66.3</b>	<b>75.10</b>

Table 2: Classification accuracy (%) on *Office-31* dataset for unsupervised domain adaptation (ResNet-50 [12])

Method	A→W	A→D	D→A	W→A	Avg
ResNet[12]	68.4	68.9	62.5	60.7	65.13
DANN[8]	82.0	79.7	68.2	67.4	74.33
MADA[30]	90.0	87.8	70.3	66.4	78.62
DAAA [16]	86.8	88.8	74.3	73.9	80.95
CDAN[25]	93.1	93.4	71.0	70.3	81.95
CAT[5]	94.4	90.8	72.2	70.2	81.90
TAT[23]	92.5	93.2	73.1	72.1	82.73
TADA [46]	94.2	92.8	72.6	73.6	83.30
CADA[19]	<b>97.0</b>	<b>95.6</b>	71.5	73.1	<b>84.30</b>
ETD[21]	92.1	88.0	71.0	67.8	79.73
DMRL[48]	90.8	93.4	73.0	71.2	82.10
ALDA[4]	95.6	94.0	72.2	72.5	83.58
DADA[40]	92.3	93.9	74.4	74.2	83.78
PMDA	91.9	93.8	72.5	74.4	83.12
CMDA	93.6	94.1	73.3	74.5	83.88
TDMDA	94.8	93.5	<b>74.7</b>	<b>75.8</b>	<b>84.70</b>

jointly satisfy:

$$(\hat{\theta}_f, \hat{\theta}_c, \hat{\theta}_g) = \arg \min_{\theta_f, \theta_c, \theta_g} J(\theta_f, \theta_c, \theta_{df}, \theta_g, \theta_{dp}, \theta_{dc}) \quad (12)$$

$$(\hat{\theta}_{df}, \hat{\theta}_{dp}, \hat{\theta}_{dc}) = \arg \max_{\theta_{df}, \theta_{dp}, \theta_{dc}} J(\theta_f, \theta_c, \theta_{df}, \theta_g, \theta_{dp}, \theta_{dc}) \quad (13)$$

## 5. Experiments and Results

### 5.1. Datasets

**Office-31** [33] dataset consists of images of office environment of three domains (Amazon, Webcam, and DSLR). It consists of 4,652 images and 31 classes. We have evaluated our model on four adaptation tasks (A→W, A→D, W→A, D→A). We removed the other two adaptation tasks (D→W, W→D) because they are very similar domains.

Table 3: Classification accuracy (%) on *ImageCLEF* dataset for unsupervised domain adaptation (ResNet-50 [12])

Method	I → PP	PP → II	II → CC	CC → IC	IC → PP	PP → C	Avg
ResNet[12]	74.8	83.9	91.5	78.0	65.5	91.2	80.7
DANN[8]	75.0	86.0	96.2	87.0	74.3	91.5	85.0
JAN[26]	76.8	88.0	94.7	89.5	74.2	91.7	85.8
MADA[30]	75.0	87.9	96.0	88.8	75.2	92.2	85.8
CDAN[25]	77.2	88.3	<b>98.3</b>	90.7	76.7	94.0	87.5
CAT[5]	77.2	91.0	95.5	91.3	75.3	93.6	87.3
TAT[23]	78.8	92.0	97.5	92.0	78.2	94.7	<b>88.9</b>
CADA[19]	78.0	90.5	96.7	92.0	77.2	95.5	88.3
DMRL[48]	77.3	90.7	97.4	91.8	76.0	94.8	88.0
AADA[50]	<b>79.2</b>	<b>92.5</b>	96.2	91.4	76.1	94.7	88.4
<b>TDMDA</b>	77.8	92.0	97.2	<b>92.7</b>	<b>78.7</b>	<b>96.2</b>	<b>89.1</b>

**Office-Home** [44] dataset consists of 65 classes with four domains Artistic (Ar), Clipart (Cl), Product (Pr) and Real-World (Rw) images. These domains are very different from each other, and adaptation is very challenging. We have reported all 12 transfer tasks for this dataset.

**ImageCLEF-2014** dataset consists of three datasets: Caltech-256 (C), ILSVRC 2012 (I), and Pascal VOC 2012 (P). There are 12 common classes, and each class has 50 samples. So, there is a total of 600 images in each domain.

## 5.2. Results

We have reported the results of the Office-31 dataset based on AlexNet in Table 1. Our method TDMDA has outperformed all of the mentioned methods by a significant margin of 4.35%. Entro [47] proposed to match the predictive uncertainty for adapting the classifier in the target domain. However, our method exceeds Entro by a large margin of 7.42% on the average accuracy. We have also reported our model performance for Office-31 dataset based on ResNet-50 in Table 2 with an improvement of 0.3%. TDMDA outperforms methods based on classifier adaptation such as TAT[23], CAT[5] and DAAA[16] by margin greater than 2%. The proposed method even performs better than the recent approaches [22, 50, 21, 4] and it also incorporates complex attention mechanisms such as [19, 46]. This shows that the adaptation of classifiers in the target domain is necessary for effective domain adaptation.

Table 4 shows the results on Office-Home dataset. This dataset is far more challenging than other datasets as domain shift is significantly high here. Despite the challenge, our method achieves a substantial improvement over the other methods across most of the tasks. TDMDA outperforms TAT[23] by a significant margin of 5.7% on average accuracy. While CADA[19] outperforms our method when Clipart (Cl) is the target domain, but the results are still competitive performing on average better than CADA.

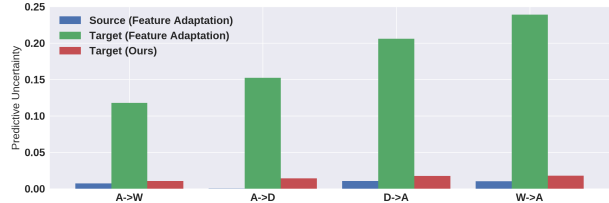


Figure 6: Predictive uncertainty in the target domain is significantly lower using our method than the adversarial feature adaptation method on *Office-31* dataset (AlexNet)

Moreover, the proposed work can be plugged with any domain adaptation framework to improve the performance further. We have also reported the results on the ImageCLEF dataset in Table 3. Our method exceeds the rest of the methods’ performance with a minor improvement of 0.2% on average accuracy. The relatively small margin in improvement is because of the smaller domain shift in the dataset.

## 5.3. Ablation Study

We have also studied the contributions of both probability distribution adaptation and certainty activation mappings adaptation. The comparison between TDMDA and its variants is reported in Table 2 for the Office-31 dataset. PMDA refers to the probability distribution adaptation, and CMDA refers to the certainty activation mapping adaptation. Results show that both PMDA and CMDA outperform most of the comparison methods. PMDA performs slightly worse than CMDA as it only encourages the classifier to learn class-discriminative feature representation with higher margins. This can lead to features aligned to incorrect class-cluster. By adapting both probability distribution along with certainty activation mapping reduces this problem. Thus, TDMDA exceeds both of them, which shows that learning both mean and variance is essential for approximating the classifier’s posterior in the target domain.

## 6. Empirical Analysis

### 6.1. Predictive Uncertainty

In figure 6, we have shown the predictive uncertainty of source and target domain after feature adaptation, and target domain after using our method (TDMDA) on the Office-31 dataset using AlexNet. We can observe that predictive uncertainty on the target domain using our approach is much less than on target domain after feature adaptation for all the tasks. This shows that the posterior of the classifier is now much better approximated for the target domain.

### 6.2. Feature Visualization

We have visualized the feature representations learned by our method TDMDA and performing only adversarial feature adaptation using t-SNE embedding [27] in figure

Table 4: Classification accuracy (%) on *Office Home* dataset for unsupervised domain adaptation (ResNet-50 [12])

Method	Ar→Cl	Ar→Pr	Ar→Rw	Cl→Ar	Cl→Pr	Cl→Rw	Pr→Ar	Pr→Cl	Pr→Rw	Rw→Ar	Rw→Cl	Rw→Pr	Avg
ResNet[12]	34.9	50.0	58.0	37.4	41.9	46.2	38.5	31.2	60.4	53.9	41.2	59.9	46.1
DANN[8]	45.6	59.3	70.1	47.0	58.5	60.9	46.1	43.7	68.5	63.2	51.8	76.8	57.6
JAN[26]	45.9	61.2	68.9	50.4	59.7	61.0	45.8	43.4	70.3	63.9	52.4	76.8	58.3
CDAN[25]	50.6	65.9	73.4	55.7	62.7	64.2	51.8	49.1	74.5	68.2	56.9	80.7	62.8
TAT[23]	51.6	69.5	75.4	59.4	69.5	68.6	59.5	50.5	76.8	70.9	56.6	81.6	65.8
TADA[46]	53.1	72.3	77.2	59.0	71.2	72.1	59.7	53.1	78.4	72.4	60.0	82.9	67.6
CADA[19]	<b>56.9</b>	76.4	80.7	61.3	75.2	75.2	63.2	<b>54.5</b>	80.7	73.9	<b>61.5</b>	84.1	70.2
ALDA[4]	53.7	70.1	76.4	60.2	72.6	71.5	56.8	51.9	77.1	70.2	56.3	82.1	66.6
AADA[50]	54.0	71.3	77.5	60.8	70.8	71.2	59.1	51.8	76.9	71.0	57.4	81.8	67.0
ETD[21]	51.3	71.9	<b>85.7</b>	57.6	69.2	73.7	57.8	51.2	79.3	70.2	57.5	82.1	67.3
DCAN[22]	54.5	75.7	81.2	<b>67.4</b>	74.0	76.3	67.4	52.7	80.6	74.1	59.1	83.5	<b>70.5</b>
TDMDA	55.4	<b>79.3</b>	81.6	64.3	<b>76.5</b>	<b>76.8</b>	<b>67.7</b>	52.2	<b>83.5</b>	<b>74.9</b>	60.4	<b>85.6</b>	<b>71.5</b>

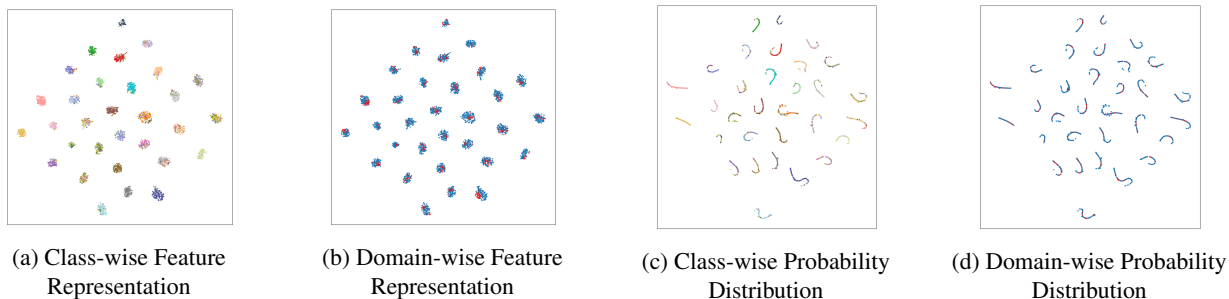


Figure 7: (a) and (b) shows t-SNE visualization of feature representations learned by TDMDA which are now class-discriminative in the target domain. (c) and (d) represents t-SNE visualization of probability distribution of TDMDA without any domain shift for Office31 dataset (Source: W and Target: A) using AlexNet.

7b and 2b for  $W \rightarrow A$  task using AlexNet respectively. Our method learns more class-discriminative feature representation and aligns most of the target domain images to a class cluster compared with features learned by feature adaptation, as observed in the figure 7a.

### 6.3. Probability Distribution Visualization

We have visualized source and target probability distributions on  $W \rightarrow A$  task on AlexNet using t-SNE embedding [27] in figures 7c and 7d. Most of the target domain’s probability distributions are now aligned to a class-cluster similar to source domain. Now there is much lesser domain shift as compared to that shown in figure 2. This provides an evidence that our method has learned a better approximation of mean  $\mu_c$  of the posterior for target domain.

### 6.4. Certainty Activation Mapping

In figure 8, we can see that after using our method, certainty activation mapping now highlights class-discriminative regions in target domain. Performing only feature adaptation does not provide class-discriminative certainty activation mappings, as shown in figure 4. This depicts the effectiveness of our method in better approxi-

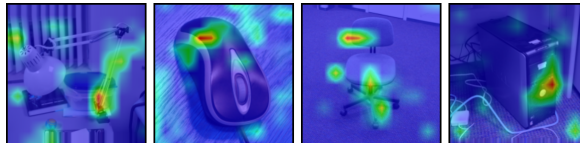


Figure 8: Visualization of certainty activation mappings using TDMDA for  $A \rightarrow D$  task (AlexNet). Certainty activation mappings are highlighting class-discriminative regions for target domain image similar to source domain

mating the posterior of the classifier in target domain.

## 7. Conclusion

In this paper, we have thoroughly analyzed the problem of matching the classifier responses between the source and target domains for successful adaptation. We observe that ignoring this aspect results in higher uncertainty in the classifier and various probability distributions being quite varied between the source and target domains. As we do not have access to the target class labels, we propose a way to indirectly ensuring that the classifier distributions are matched by the triple distribution matching approach. Our thorough empirical analysis demonstrates that this does

indeed result in improved performance and lower the uncertainty for domain adaptation. Moreover, as the eventual goal is classification, it is therefore more pertinent to consider the classifier response in a more comprehensive way as we show in this work.

## References

- [1] Charles Blundell, Julien Cornebise, Koray Kavukcuoglu, and Daan Wierstra. Weight uncertainty in neural network. In *International Conference on Machine Learning*, pages 1613–1622, 2015.
- [2] Konstantinos Bousmalis, Nathan Silberman, David Dohan, Dumitru Erhan, and Dilip Krishnan. Unsupervised pixel-level domain adaptation with generative adversarial networks. In *The IEEE Conference on Computer Vision and Pattern Recognition (CVPR)*, volume 1, page 7, 2017.
- [3] Liang-Chieh Chen, George Papandreou, Iasonas Kokkinos, Kevin Murphy, and Alan L Yuille. Deeplab: Semantic image segmentation with deep convolutional nets, atrous convolution, and fully connected crfs. *IEEE transactions on pattern analysis and machine intelligence*, 40(4):834–848, 2017.
- [4] Minghao Chen, Shuai Zhao, Haifeng Liu, and Deng Cai. Adversarial-learned loss for domain adaptation. In *AAAI*, pages 3521–3528, 2020.
- [5] Zhijie Deng, Yucen Luo, and Jun Zhu. Cluster alignment with a teacher for unsupervised domain adaptation. In *Proceedings of the IEEE International Conference on Computer Vision*, pages 9944–9953, 2019.
- [6] Yarin Gal. *Uncertainty in Deep Learning*. PhD thesis, University of Cambridge, 2016.
- [7] Yarin Gal and Zoubin Ghahramani. Dropout as a bayesian approximation: Representing model uncertainty in deep learning. In *international conference on machine learning*, pages 1050–1059, 2016.
- [8] Yaroslav Ganin and Victor Lempitsky. Unsupervised domain adaptation by backpropagation. In *International Conference on Machine Learning*, pages 1180–1189, 2015.
- [9] Yaroslav Ganin, Evgeniya Ustinova, Hana Ajakan, Pascal Germain, Hugo Larochelle, François Laviolette, Mario Marchand, and Victor Lempitsky. Domain-adversarial training of neural networks. *The Journal of Machine Learning Research*, 17(1):2096–2030, 2016.
- [10] Ian Goodfellow, Jean Pouget-Abadie, Mehdi Mirza, Bing Xu, David Warde-Farley, Sherjil Ozair, Aaron Courville, and Yoshua Bengio. Generative adversarial nets. In *Advances in neural information processing systems*, pages 2672–2680, 2014.
- [11] Chuan Guo, Geoff Pleiss, Yu Sun, and Kilian Q Weinberger. On calibration of modern neural networks. In *International Conference on Machine Learning*, pages 1321–1330, 2017.
- [12] Kaiming He, Xiangyu Zhang, Shaoqing Ren, and Jian Sun. Deep residual learning for image recognition. In *Proceedings of the IEEE conference on computer vision and pattern recognition*, pages 770–778, 2016.
- [13] Judy Hoffman, Eric Tzeng, Taesung Park, Jun-Yan Zhu, Phillip Isola, Kate Saenko, Alexei Efros, and Trevor Darrell. Cycada: Cycle-consistent adversarial domain adaptation. In *International Conference on Machine Learning*, pages 1994–2003, 2018.
- [14] Lanqing Hu, Meina Kan, Shiguang Shan, and Xilin Chen. Duplex generative adversarial network for unsupervised domain adaptation. In *The IEEE Conference on Computer Vision and Pattern Recognition (CVPR)*, June 2018.
- [15] Haoshuo Huang, Qixing Huang, and Philipp Krahenbuhl. Domain transfer through deep activation matching. In *Proceedings of the European Conference on Computer Vision (ECCV)*, September 2018.
- [16] Guoliang Kang, Liang Zheng, Yan Yan, and Yi Yang. Deep adversarial attention alignment for unsupervised domain adaptation: the benefit of target expectation maximization. In *Proceedings of the European Conference on Computer Vision (ECCV)*, pages 401–416, 2018.
- [17] Alex Kendall and Yarin Gal. What uncertainties do we need in bayesian deep learning for computer vision? In *Advances in neural information processing systems*, pages 5574–5584, 2017.
- [18] Alex Krizhevsky, Ilya Sutskever, and Geoffrey E Hinton. Imagenet classification with deep convolutional neural networks. In *Advances in neural information processing systems*, 2012.
- [19] Vinod Kumar Kurmi, Shanu Kumar, and Vinay P. Namboodiri. Attending to discriminative certainty for domain adaptation. In *The IEEE Conference on Computer Vision and Pattern Recognition (CVPR)*, June 2019.
- [20] Seungmin Lee, Dongwan Kim, Namil Kim, and Seong-Gyun Jeong. Drop to adapt: Learning discriminative features for unsupervised domain adaptation. In *Proceedings of the IEEE International Conference on Computer Vision*, pages 91–100, 2019.
- [21] Mengxue Li, Yi-Ming Zhai, You-Wei Luo, Peng-Fei Ge, and Chuan-Xian Ren. Enhanced transport distance for unsupervised domain adaptation. In *Proceedings of the IEEE/CVF Conference on Computer Vision and Pattern Recognition*, pages 13936–13944, 2020.
- [22] Shuang Li, Chi Harold Liu, Qiuxia Lin, Binhui Xie, Zhengming Ding, Gao Huang, and Jian Tang. Domain conditioned adaptation network. In *AAAI*, pages 11386–11393, 2020.
- [23] Hong Liu, Mingsheng Long, Jianmin Wang, and Michael Jordan. Transferable adversarial training: A general approach to adapting deep classifiers. In *International Conference on Machine Learning*, pages 4013–4022, 2019.
- [24] Mingsheng Long, Yue Cao, Jianmin Wang, and Michael Jordan. Learning transferable features with deep adaptation networks. In *International Conference on Machine Learning*, pages 97–105, 2015.
- [25] Mingsheng Long, Zhangjie Cao, Jianmin Wang, and Michael I Jordan. Conditional adversarial domain adaptation. In *Advances in Neural Information Processing Systems*, pages 1647–1657, 2018.
- [26] Mingsheng Long, Han Zhu, Jianmin Wang, and Michael I Jordan. Deep transfer learning with joint adaptation networks. In *International Conference on Machine Learning*, pages 2208–2217, 2017.

- [27] Laurens van der Maaten and Geoffrey Hinton. Visualizing data using t-sne. *Journal of machine learning research*, 9(Nov):2579–2605, 2008.
- [28] Yaniv Ovadia, Emily Fertig, Jie Ren, Zachary Nado, David Sculley, Sebastian Nowozin, Joshua Dillon, Balaji Lakshminarayanan, and Jasper Snoek. Can you trust your model’s uncertainty? evaluating predictive uncertainty under dataset shift. In *Advances in Neural Information Processing Systems*, pages 13991–14002, 2019.
- [29] Vishal M Patel, Raghuraman Gopalan, Ruonan Li, and Rama Chellappa. Visual domain adaptation: A survey of recent advances. *IEEE signal processing magazine*, 32(3):53–69, 2015.
- [30] Zhongyi Pei, Zhangjie Cao, Mingsheng Long, and Jianmin Wang. Multi-adversarial domain adaptation. In *Thirty-Second AAAI Conference on Artificial Intelligence*, 2018.
- [31] Shaoqing Ren, Kaiming He, Ross Girshick, and Jian Sun. Faster r-cnn: Towards real-time object detection with region proposal networks. In *Advances in neural information processing systems*, pages 91–99, 2015.
- [32] Carlos Riquelme, George Tucker, and Jasper Snoek. Deep bayesian bandits showdown: An empirical comparison of bayesian deep networks for thompson sampling. In *International Conference on Learning Representations*, 2018.
- [33] Kate Saenko, Brian Kulis, Mario Fritz, and Trevor Darrell. Adapting visual category models to new domains. In *European conference on computer vision*, pages 213–226. Springer, 2010.
- [34] Swami Sankaranarayanan, Yogesh Balaji, Carlos D Castillo, and Rama Chellappa. Generate to adapt: Aligning domains using generative adversarial networks. In *Proceedings of the IEEE Conference on Computer Vision and Pattern Recognition*, pages 8503–8512, 2018.
- [35] Ramprasaath R Selvaraju, Michael Cogswell, Abhishek Das, Ramakrishna Vedantam, Devi Parikh, Dhruv Batra, et al. Grad-cam: Visual explanations from deep networks via gradient-based localization. In *ICCV*, pages 618–626, 2017.
- [36] Jian Shen, Yanru Qu, Weinan Zhang, and Yong Yu. Adversarial representation learning for domain adaptation. *arXiv preprint arXiv:1707.01217*, 2017.
- [37] Jian Shen, Yanru Qu, Weinan Zhang, and Yong Yu. Wasserstein distance guided representation learning for domain adaptation. In *AAAI*, 2018.
- [38] Rui Shu, Hung H Bui, Hirokazu Narui, and Stefano Ermon. A dirt-t approach to unsupervised domain adaptation. In *Proc. 6th International Conference on Learning Representations*, 2018.
- [39] Baochen Sun and Kate Saenko. Deep coral: Correlation alignment for deep domain adaptation. In *European Conference on Computer Vision*, pages 443–450. Springer, 2016.
- [40] Hui Tang and Kui Jia. Discriminative adversarial domain adaptation. In *AAAI*, pages 5940–5947, 2020.
- [41] Eric Tzeng, Judy Hoffman, Trevor Darrell, and Kate Saenko. Simultaneous deep transfer across domains and tasks. In *Computer Vision (ICCV), 2015 IEEE International Conference on*, pages 4068–4076. IEEE, 2015.
- [42] Eric Tzeng, Judy Hoffman, Kate Saenko, and Trevor Darrell. Adversarial discriminative domain adaptation. In *Computer Vision and Pattern Recognition (CVPR)*, volume 1, page 4, 2017.
- [43] Eric Tzeng, Judy Hoffman, Ning Zhang, Kate Saenko, and Trevor Darrell. Deep domain confusion: Maximizing for domain invariance. *arXiv preprint arXiv:1412.3474*, 2014.
- [44] Hemanth Venkateswara, Jose Eusebio, Shayok Chakraborty, and Sethuraman Panchanathan. Deep hashing network for unsupervised domain adaptation. In *Proc. CVPR*, pages 5018–5027, 2017.
- [45] Mei Wang and Weihong Deng. Deep visual domain adaptation: A survey. *Neurocomputing*, 2018.
- [46] Ximei Wang, Liang Li, Weirui Ye, Mingsheng Long, and Jianmin Wang. Transferable attention for domain adaptation. In *Thirty-Third AAAI Conference on Artificial Intelligence*, 2019.
- [47] Jun Wen, Nenggan Zheng, Junsong Yuan, Zhefeng Gong, and Changyou Chen. Bayesian uncertainty matching for unsupervised domain adaptation. In *Proceedings of the 28th International Joint Conference on Artificial Intelligence*, pages 3849–3855. AAAI Press, 2019.
- [48] Yuan Wu, Diana Inkpen, and Ahmed El-Roby. Dual mixup regularized learning for adversarial domain adaptation. *ECCV*, 2020.
- [49] Hongliang Yan, Yukang Ding, Peihua Li, Qilong Wang, Yong Xu, and Wangmeng Zuo. Mind the class weight bias: Weighted maximum mean discrepancy for unsupervised domain adaptation. In *Proceedings of the IEEE Conference on Computer Vision and Pattern Recognition*, pages 2272–2281, 2017.
- [50] Jianfei Yang, Han Zou, Yuxun Zhou, Zhaoyang Zeng, and Lihua Xie. Mind the discriminability: Asymmetric adversarial domain adaptation. *ECCV*, 2020.